Rapid Communications

Bulk-boundary correspondence in soft matter

Mehmet Ramazanoglu [1,2,*] Şener Özönder,[1,3,†] and Rumeysa Salcı[1]

[1]*Physics Engineering Department, Istanbul Technical University, 34469 Maslak, Istanbul, Turkey*
[2]*Brockhouse Institute for Materials Research, Hamilton, Ontario, Canada L8S 4M1*
[3]*Department of Electrical and Electronics Engineering, Istinye University, 34010, Istanbul, Turkey*

Bulk-boundary correspondence is the emergence of features at the boundary of a material that are dependent on and yet distinct from the properties of the bulk of the material. The diverse applications of this idea in topological insulators as well as high energy physics prove its universality. However, whether a form of bulk-boundary correspondence holds also in soft matter such as gels, polymers, lipids, and other biomaterials is thus far unknown. Aerosil-dispersed liquid crystal gels provide a good testing ground to explore the relation between the controlled variations of the aerosil density within the liquid crystal bulk and the surface topography of the sample. Here we report on a direct observation of such a correspondence where the controlled strength of random disorder created by aerosil dispersion in the bulk liquid crystal is correlated with the fractal dimension of the surface. We obtained the surface topography of our gel samples with different quenched random disorder strengths by using atomic force microscope techniques, and computed the fractal dimension for each sample. We found that an increase of the aerosil gel density in the bulk corresponds to an increase in the fractal dimension at the surface. From our results emerges a method to acquire the bulk properties of soft matter such as density, randomness, and phase merely from the fractal dimension of the surface.

The connection between a material's bulk and its boundary has been one of the guiding principles in several branches of physics in the last decade. The main idea is that the boundary of the system would feature excitations that do not occur in the bulk, yet the physics on the boundary is still determined by the properties of the bulk. For example, in topological insulators, the index theorem relates the Chern number quantifying the topology of the insulating bulk to the spectrum of the edge states at the boundary [1–4]. The holographic principle in high energy physics, also known as gauge-gravity duality, is another example of the bulk-boundary correspondence where the spectrum of the strongly interacting gauge theory in four space-time dimensions is connected to the weakly interacting theory on the three-dimensional boundary via duality [5,6].

Here we report on a test of whether bulk-boundary correspondence holds in soft condensed matter systems [7,8], particularly in aerosil-dispersed liquid crystals [Fig. 1(a)]. We prepared liquid crystal+aerosil (LC+aerosil) gel mixtures with varying amounts of aerosil within, and observed that the aerosil gel density $\rho_s = m_{SiO_2}/V_{LC}$ in the bulk is correlated with the fractal dimension of the surface. This experimental verification of the bulk-boundary correspondence in soft matter is the main goal of this study.

Liquid crystals (LCs) are not only utilized in screens and TVs, but also used to study phase transitions [9]. Since they possess a rich spectrum of different phases with different types of phase transitions, they stand out as particular model systems where not only structural but also magnetic phase transitions can be imitated. Pure and doped LCs can mimic complex many-body systems such as quantum magnets in random background fields. Having two order parameters, amplitude ψ and phase α, make LCs unique materials that closely resemble superconductors [9]. There is a strong mapping between different LC phases and the phases of the nematic spin order of the antiferromagnetic modulations in Fe-As–based metals and superconductors. Thus, LCs are used to simulate and better understand certain solid-state materials [10].

Aerosil nanoparticles dispersed in LC hosts lead to a random network of locally pinned LC molecules, thus they can be used to study the controlled random disorder effects and the associated phase transitions [11–23]. The electrostatic interaction between the aerosil surface and the polar end of the LC molecules creates pinning forces that perturb the order in the nematic and smectic LC layers [Fig. 1(b)]. Since the position of the aerosil nanoparticles are random in the LC bulk, the resultant random perturbation of LC order becomes quenched, a situation which is known as quenched random disorder [12,15,22].

With heat-capacity measurements and x-ray scattering experiments, the quenched random disorder effects on the phase transition characteristics for several LCs were studied within nematic and smectic phases.

Aerosil dispersion within LCs not only creates quenched random disorder in the bulk, but also causes topographical changes on the material's surface. For example, increasing aerosil gel density within the sample makes its surface rougher [24,25]. Physical systems where the structural randomness can be controlled, hereby varying the aerosil gel density ρ_s, also appear in solid-state physics. One example that has been examined in random-field experiments is $MnZnF_2$. $MnZnF_2$

_____

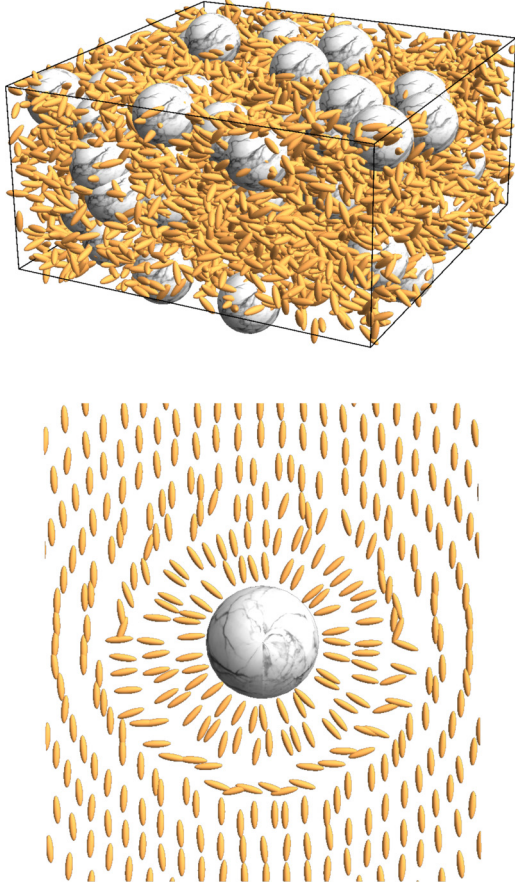*ramazanoglum@itu.edu.tr
†ozonder@uw.edu

FIG. 1. Aerosil and liquid crystal (LC) mixture. Top: A 3D cartoon of dispersed aerosil nanoparticles in LCs. Bottom: The hydroxyl groups covering the surface of aerosils, which are 7 nm in diameter, electrostatically interact with 8CB LC molecules. This disturbs the nematic or smectic order. Since the aerosil nanoparticles form a random network, the LC phase perturbation becomes random as well.

is a diluted quantum antiferromagnet where its magnetic properties can be explained by the three-dimensional (3D) random-field Ising model. Here the long-range order of the antiferromagnetic interactions is disrupted by the doped nonmagnetic Zn ions, and the remaining short-range antiferromagnetic phase can be controlled by an external field [26].

Random pinning of aerosil particles in the bulk changes the surface while they introduce short-range modulations in the nematic and smectic phases in the bulk structure [24,25]. Therefore the randomness in the bulk reflects itself as a self-affine, fractal surface on the boundary. In order to test this relation between the bulk and surface, we prepared seven LC+aerosil (8CB+SiO$_2$) gel mixtures with $\rho_s = 0.051$, 0.078, 0.104, 0.22, 0.347, 0.49 and 0.647 g/cm^3. Here 8CB is the abbreviation for octylcyanobiphenyl LC. Since aerosil nanoparticles disrupt the ordered state of LCs, the strength of quenched random disorder in the bulk of 8CB LCs can be controlled by adjusting the aerosil gel density ρ_s. This parameter has also been used to characterize the LC+aerosil gel samples [11–22,25].

We scanned the surfaces of our samples with an atomic force microscope (AFM) and obtained surface height

profiles with nanometer precision into 256×256 matrices [25]. From the surface data, we first compute the surface fractal dimension D_F of each sample and then investigate if D_F's are correlated with ρ_s's, which are known for each sample.

I. METHODS

In this study, we used 8CB LCs (Frinton Laboratories) without purification process as they have been used in previous x-ray and heat capacity experiments [14,16,17]. Our hydrophilic aerosils (Evonik Corporation) were type 300 silica nanoparticles which were ~7 nm in diameter. The Brunauer-Emmet-Teller surface area for these nanoparticles is listed by the producer as 300 m^2 g^{-1}. Before mixing with 8CB LC, the aerosil was dried at elevated temperatures of $T \sim 500$ K under a vacuum of $\sim 10^{-2}$ atm for more than a week. The LC+aerosil mixtures were prepared according to stoichiometric ratios using the density equation $\rho_s = m_{\mathrm{aerosil}}/V_{\mathrm{LC}}$. This value can be obtained from $\rho_s^{-1} = \rho^{-1} - \rho_{\mathrm{aerosil}}^{-1}$ where ρ_{aerosil} is 2.2 g/cm^3. Here ρ is the ratio of the aerosil mass to the total volume of the sample, and ρ_s is the aerosil gel density. This parameter is used to define the strength of the disorder effects created by aerosil dispersion in LC [14,18–20,25]. The aerosil nanoparticles were mixed with high-purity ethanol. Each sample was sonicated at ~300 K for 30 min. These liquid mixtures were then placed on a hot plate for the gelation process. The temperature was held in the vicinity of 8CB's isotropic phase temperature $\sim 310 \pm 0.5$ K so that all samples were dried in the isotropic phase.

The gelation process takes several days depending on the amount of aerosil mass in the mixture. The gel samples prepared with the low concentration of $\rho_s \lesssim 0.347$ g/cm^3 were placed on Si wafers using a spatula which was held at ~310 K, the same as the drying process temperature. The samples on the Si wafers were then relaxed again at the drying temperature on the hot plate for ~24 h. For the two highest ρ_s concentrations in Table I, the drying process produced small cracks on the sample surfaces. These samples were transferred to the Si surface using warm tweezers held

TABLE I. Aerosil gel densities and fractal dimensions of the samples. Aerosil gel density ρ_s, weight percentage wt %, fractal dimensions obtained from the box counting, coarse-graining and power spectral density techniques, and the order parameter β are given. Here the aerosil gel density ρ_s is given by $\rho_s = m_{\mathrm{aerosil}}/V_{\mathrm{LC}}$ in units of g/cm^3, and it also quantifies the strength of disorder in the bulk. The weight percentage wt % can likewise be used to quantify the disorder strength. The values of β are known from x-ray scattering experiments [14,16].

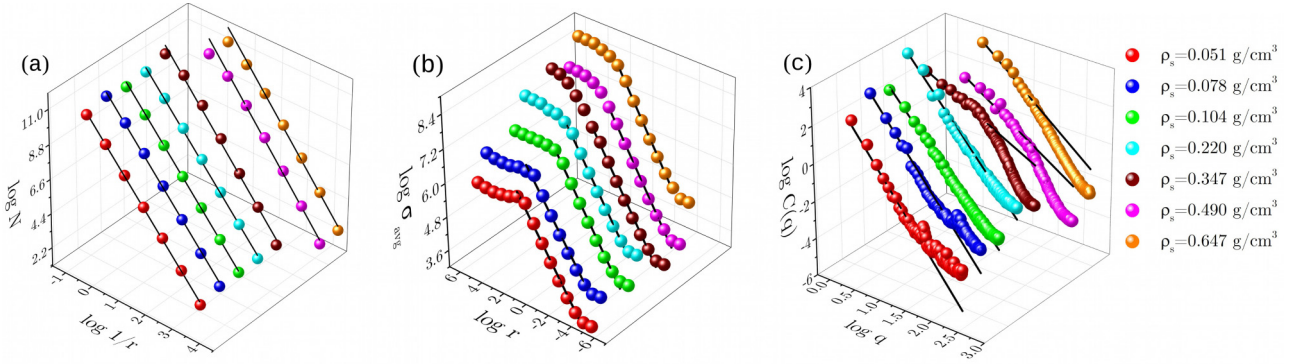| ρ_s	wt %	D_F^{box}	D_F^{CG}	D_F^{PSD}	β
0.051	4.9	2.02(2)	0.59(5)	2.12(4)	0.22(2)
0.078	7.3	1.99(5)	0.66(4)	2.24(3)	0.23(2)
0.104	9.5	2.04(2)	0.69(2)	2.44(4)	0.26(2)
0.22	18	2.10(4)	0.70(2)	2.39(8)	0.31(2)
0.347	26	2.29(6)	0.72(2)	2.72(3)	0.28(4)
0.49	33	2.25(8)	0.73(2)	2.88(3)	0.39(3)
0.647	39.5	2.23(8)	0.75(1)	2.85(5)	0.41(3)

FIG. 2. Fractal dimension analysis of LC+aerosil gel surfaces. (a) Box counting, (b) coarse-graining, and (c) power spectral density calculations and associated power-law fits are shown in log-log plots. There are seven sets of data within each plot which correspond to our seven samples with different aerosil gel densities ρ_s.

again at ~307 K. The samples were carefully held at the drying temperature during the transfer and they were relaxed after the transfer process lest the LC+aerosil gel network be externally disturbed or thermally stressed. Thus, high-quality 8CB+aerosil samples were prepared carefully without any undesirable crystallization or phase separation issues.

The AFM scans were conducted at the Nanotechnology Research Center (ITUnano) at Istanbul Technical University, a clean room facility where the temperature and humidity were held constant at 296 K and ~35%, respectively. This temperature is just 6 K over the crystallization temperature of the pure 8CB; therefore, we avoided any unwanted accidental crystallization during the surface scans. The scan area for $\rho_s = 0.051, 0.078, 0.104, 0.22,$ and 0.347 g/cm^3 was 5 μm^2, and for $\rho_s = 0.49$ and 0.647 g/cm^3 it was 2 μm^2. The 3D surface pictures can be found elsewhere [25].

The AFM (Nanomagnetics) was used in noncontact mode at a frequency of ~161 kHz. The AFM scans were transferred to MATLAB and *Mathematica* using NMI Image Analyzer v1.4 software. All of the surface analyses described in the main text were performed using our own codes.

II. ANALYSIS

Fractal surfaces appear in nature in diverse areas such as fracture in rocks, cancer growth processes, wetting of surfaces, burning of paper, and rupturing [27,28]. Fractal surfaces possess self-affine structure, i.e., when observed at different scales the surface looks self-similar. This scale-independent property is characterized by fractal dimension D_F, which is calculated from the variation of the surface roughness with respect to the spatial scale. We use three separate methods to calculate fractal dimension of our samples' surfaces: power spectral density, box counting, and coarse-graining (also called variable bandwidth) [Figs. 2(a)–2(c)]. Since the value of the fractal dimension is dependent on the method used, each method has its own definition of fractal dimension and its own systematic and random errors. In this work, we are interested in the trend of how D_F changes with varying aerosil gel density ρ_s rather than the actual values of the fractal dimensions of each sample.

Before calculating D_F's, we created, with simulation, mock fractal surfaces with known D_F's in order to test our codes,

and from these simulations we determined systematic and random errors of the three methods we used to calculate D_F's. Then we used our codes on the real AFM surface data from our samples and our findings established that our fractal dimension analysis data from all three D_F calculation methods fall on a straight line on a log-log plot [Figs. 2(a)–2(c)]. This power-law feature indicates the existence of self-affine surface structure and makes the use of fractional dimension analysis justified.

One of the methods we used to calculate D_F's of the surfaces is power spectral density (PSD). We calculated the periodograms, i.e., Fourier transform squared, for each surface data. We verified that periodograms of our data fall as power law in inverse length scale, which is characteristic of a self-affine surface. The slope of the fall-off in the Fourier space gives D_F^{PSD} of that surface. The fits have been performed with the data points at the lower end of the power spectrum, from the first to the 25th Fourier mode. This is due to the fact that in power-law type spectra, the greatest amplitudes appear in the lower end of the spectrum whereas contributions from the higher modes are negligible. When we plot D_F versus ρ_s, we find a rising trend where D_F increases with increasing aerosil density ρ_s [Fig. 2(a)]. We find a similar trend by using the box counting method [Fig. 2(b)]. For this method, we first turned our surface height data from 256×256 matrices into 3D arrays of 256×256×256 by rescaling the surface heights between 1 and 256. This gives us 3D arrays that contain 1's at coordinates that correspond to the surface heights and 0's for the remaining entries. Then we divide these 3D arrays into boxes of size $r = 2, 4, 8, 16, 32, 64,$ and 128, and count the number of boxes containing 1's for each r, which we call $n(r)$. We find box counting dimension D_F^{box} by fitting our counts to the curve $n(r) = r^{-D_F^{box}}$. The third method we employed was the coarse-graining (CG) method where we first turn the 256×256 surface data into a one-dimensional list by flattening it. Then we divide this list into equal partitions of size r. For a chosen r, we calculate the standard deviation σ of the heights within each partition, and calculate the mean of those σ's to find σ_{avg}. We repeat this calculation for different values of partition size r, which are different powers of 2. The coarse-graining fractal dimension D_F^{CG} is found by fitting the curve $\sigma_{avg}(r) = r^{\zeta}$ to the calculated σ_{avg} values, and then using the definition $D_F^{CG} = 2 + \zeta$. The coarse-graining
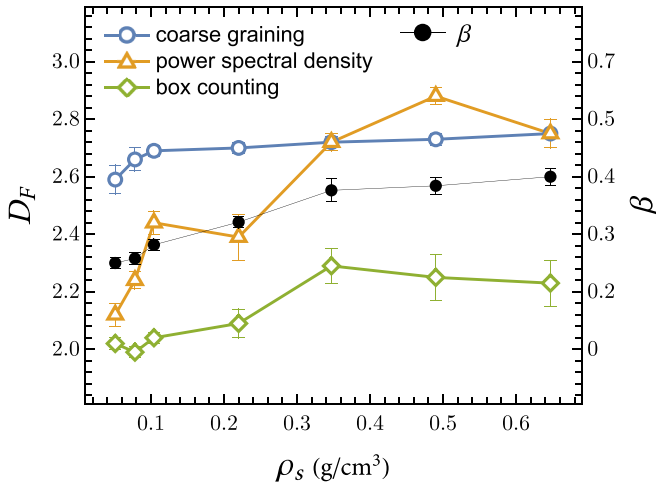
FIG. 3. Correlation between the aerosil gel density, the fractal dimension, and the order parameter β. Calculated fractal dimensions with respect to aerosil gel density ρ_s, which controls the disorder strength in the bulk. This graph also contains the order parameter β values obtained from previous x-ray experiments [14,17,19]. We added "2" to the order parameter β to be able to show all of the results on the same graph. The error bars are coming from the Marquardt-Levenberg nonlinear fit analyses.

method yields an increasing trend similar to the other two methods [Fig. 2(c)]. Here we emphasize that we have made our fits to extract D_F's for each sample by using the same range of data points within all three methods, otherwise one can find any trend by arbitrarily choosing the fit range (see Supplemental Material figures for the detailed plots of all the fits [29]).

III. RESULTS

The results of this study (Table I) establish a positive correlation between the bulk aerosil gel density ρ_s and the surface fractal dimension D_F. Figure 3 shows that the surface fractal dimension, calculated via three different methods, increases with increasing ρ_s.

Since ρ_s also controls the strength of the randomness in the bulk, the bulk-boundary correspondence we discovered also reveals a link between the surface fractality and the order parameter β measured via x-ray scattering. The parameter β is the order parameter exponent which was obtained from the x-ray scattering fits [14,17] and it demonstrates the characteristic changes in the smectic modulations with aerosil dispersion. In Fig. 3, in addition to D_F's, we also show the trend of the order parameter β versus the aerosil gel density ρ_s, which can also be seen as the disorder strength. According

to previous x-ray studies, β exhibits an increasing trend with respect to increasing ρ_s. The smaller β values fall into the universality class of the two-dimensional Ising model. As ρ_s increases, the increasing β values go past the tricritical point and become equal to that of the universality class of the 3D Ising model [14,20,22]. Such an increase in β is a sign of change in the universality class of the 8CB LC's smectic-A phase under the quenched random disorder effects. Our findings (Fig. 3) uncover the correlation between the order parameter β and the fractal dimension D_F.

Our results are also in good agreement with the 3D colloidal fractal dimension values obtained from small-angle x-ray scattering (SAXS) measurements [30]. Silica colloid clusters in solution have been studied via electron microscopy, light scattering, and SAXS techniques. Unlike our measurements, these experiments directly measure the bulk characteristics such as the order parameter β in the x-ray LC scattering measurements. The D_F values obtained from these measurements are found to be in the vicinity of $D_F \sim 2$ for the samples with low silica content. In these experiments, fine powders of silica are compressed in order to increase the silica density. As in the case of our high ρ_s samples, a similar increase in the calculated fractal colloid dimension has been observed at high silica densities where the fractal dimension reaches $D_F \sim 2.5$ [30].

The gels of LC+aerosil mixtures can create systems with controlled random disorder, and our experiments have demonstrated that this randomness in the bulk reflects itself at the boundary as fractal surfaces. This reveals the interconnection between the aerosil gel density in bulk ρ_s, order parameter β, and surface fractal dimension D_F. It remains an open question as to which other soft materials would feature such a bulk-boundary correspondence. In this work we used LCs to verify the existence of the bulk-boundary correspondence in soft matter, which can be seen as a proof of concept study. On the other hand, a research program dedicated to investigating the interplay between D_F and the properties of other soft materials such as polymers, gels, lipids, and other biomaterials is needed. Furthermore, theoretical studies to understand the exact mechanisms that lead to bulk-boundary correspondence in randomly disordered soft matter are also missing. This line of research may open the door to engineering surfaces of polymers and biomaterials by controlling bulk randomness in order to obtain the desired surface wetting and friction properties, which mainly depend on surface fractality.

[1] M. Z. Hasan and C. L. Kane, Colloquium: Topological insulators, Rev. Mod. Phys. **82**, 3045 (2010).

[2] X.-L. Qi and S.-C. Zhang, Topological insulators and superconductors, Rev. Mod. Phys. **83**, 1057 (2011).

[3] C. Kane, Topological band theory and the $\mathbb{Z}2$ invariant, in *Topological insulators*, Contemporary Concepts of Condensed Matter Science Vol. 6 (Elsevier, New York, 2013), Chap. 1, pp. 3–34.

[4] T. E. Lee, Anomalous Edge State in a Non-Hermitian Lattice, Phys. Rev. Lett. **116**, 133903 (2016).

[5] H. Liu, From black holes to strange metals, Phys. Today **65**(6), 68 (2012).

[6] R. Bousso, The holographic principle, Rev. Mod. Phys. **74**, 825 (2002).

[7] E. M. Terentjev and D. A. Weitz, *The Oxford handbook of soft condensed matter* (Oxford University Press, New York, 2017).

[8] M. Kleman and O. D. Laverntovich, *Soft matter physics: An introduction* (Springer Science & Business Media, Berlin, 2007).

[9] P. G. de Gennes and J. Prost, *The Physics of Liquid Crystals*, 2nd ed. (Oxford Science Publications, New York, 2003).

[10] Q. Zhang, R. M. Fernandes, J. Lamsal, J. Yan, S. Chi, G. S. Tucker, D. K. Pratt, J. W. Lynn, R. W. McCallum, P. C. Canfield, T. A. Lograsso, A. I. Goldman, D. Vaknin, and R. J. McQueeney, Neutron-Scattering Measurements of Spin Excitations in LaFeAsO and Ba(Fe$_{0.953}$Co$_{0.047}$)$_2$As$_2$ Evidence for a Sharp Enhancement of Spin Fluctuations by Nematic Order, Phys. Rev. Lett. **114**, 057001 (2015).

[11] B. Zhou, G. Iannacchione, and C. Garland, Calorimetric study of phase transitions for octylphenylthiolpentyloxybenzoate in silica aerogels, Liq. Crys. **22**, 335 (1997).

[12] H. Haga and C. W. Garland, Effect of silica aerosil particles on liquid-crystal phase transitions, Phys. Rev. E **56**, 3044 (1997).

[13] G. S. Iannacchione, C. W. Garland, J. T. Mang, and T. P. Rieker, Calorimetric and small angle x-ray scattering study of phase transitions in octylcyanobiphenyl-aerosil dispersions, Phys. Rev. E **58**, 5966 (1998).

[14] S. Park, R. L. Leheny, R. J. Birgeneau, J.-L. Gallani, C. W. Garland, and G. S. Iannacchione, Hydrogen-bonded silica gels dispersed in a smectic liquid crystal: A random field XY system, Phys. Rev. E **65**, 050703 (2002).

[15] T. Bellini, M. Buscaglia, C. Chiccoli, F. Mantegazza, P. Pasini, and C. Zannoni, Nematics with Quenched Disorder: What is Left when Long Range Order is Disrupted?, Phys. Rev. Lett. **85**, 1008 (2000).

[16] R. L. Leheny, S. Park, R. J. Birgeneau, J.-L. Gallani, C. W. Garland, and G. S. Iannacchione, Smectic ordering in liquid-crystal–aerosil dispersions. I. X-ray scattering, Phys. Rev. E **67**, 011708 (2003).

[17] G. S. Iannacchione, S. Park, C. W. Garland, R. J. Birgeneau, and R. L. Leheny, Smectic ordering in liquid-crystal–aerosil dispersions. II. Scaling analysis, Phys. Rev. E **67**, 011709 (2003).

[18] M. Ramazanoglu, S. Larochelle, C. W. Garland, and R. J. Birgeneau, High-resolution x-ray scattering study of the effect of quenched random disorder on the nematic–smectic-A transition, Phys. Rev. E **75**, 061705 (2007).

[19] M. K. Ramazanoglu, P. S. Clegg, R. J. Birgeneau, C. W. Garland, M. E. Neubert, and J. M. Kim, First-order isotropic–smectic-A transition in liquid-crystal–aerosil gels, Phys. Rev. E **69**, 061706 (2004).

[20] M. Ramazanoglu, S. Larochelle, C. W. Garland, and R. J. Birgeneau, High-resolution x-ray study of nematic–smectic-A and smectic-A–reentrant-nematic transitions in liquid-crystal–aerosil gels, Phys. Rev. E **77**, 031702 (2008).

[21] B. Freelon, M. Ramazanoglu, P. J. Chung, R. N. Page, Y. T. Lo, P. Valdivia, C. W. Garland, and R. J. Birgeneau, Smectic-A and smectic-C phases and phase transitions in $\bar{8}S5$ liquid-crystal–aerosil gels, Phys. Rev. E **84**, 031705 (2011).

[22] C. W. Garland and G. Nounesis, Critical behavior at nematic–smectic-A phase transitions, Phys. Rev. E **49**, 2964 (1994).

[23] T. Bellini, L. Radzihovsky, J. Toner, and N. A. Clark, Universality and scaling in the disordering of a smectic liquid crystal, Science **294**, 1074 (2001).

[24] A. Hauser, H. Kresse, A. Glushchenko, and O. Yaroshchuk, AFM investigations of a glassy cholesteric liquid crystal with hydrophobic aerosil particles, Liq. Cryst. **26**, 1603 (1999).

[25] R. Salci, D. A. Acar, O. Oztirpan, and M. Ramazanoglu, A new probe: AFM measurements for random disorder systems, Chin. Phys. Lett. **36**, 010501 (2019).

[26] R. Birgeneau, Y. Shapira, G. Shirane, R. Cowley, and H. Yoshizawa, Random fields and phase transitions, Physica B+C **137**, 83 (1986).

[27] B. N. J. Persson, O. Albohr, U. Tartaglino, A. I. Volokitin, and E. Tosatti, On the nature of surface roughness with application to contact mechanics, sealing, rubber friction and adhesion, J. Phys.: Condens. Matter **17**, R1 (2005).

[28] A.-L. Barabsi and H. E. Stanley, *Fractal concepts in surface growth* (Cambridge University Press, Cambridge, UK, 1995).

[29] See Supplemental Material at http://link.aps.org/supplemental/10.1103/PhysRevE.100.020702 for the detail fits of the analyses used in this work.

[30] J. Feder, *Fractals* (Springer, US, 1988).